Structural Studies and Solution Dynamics of Complexes of Magnesium with the *N,N*-Dimethylaminomethylferrocenyl Ligand

Naka Seidel,[a] Klaus Jacob,*[a] Axel K. Fischer,[b] Claus Pietzsch,[c] Pierro Zanello,[d] and Marco Fontani[d]

Keywords: Chelates / Chirality / Cyclic voltammetry / Magnesium / Moessbauer spectroscopy

The reaction of {*C,N*-[Fe(η^5-C_5H_5)(η^5-C_5H_3(CH_2NMe_2)-2)]}Li, (FcN)Li, with magnesium bromide affords the magnesate complex $Li_2Mg(FcN)_2Br_2(OEt_2)_2$ **(1)**. Extraction of **1** with diethyl ether yields $(FcN)_2Mg(OEt_2)$ **(2).** The reaction of (FcN)Li with magnesium halides and THF directly affords $(FcN)_2Mg(THF)$ **(3)**. In solution, these compounds appear as a mixture of diastereomers, whereas in the solid state they each crystallize as a single *rac*-diastereomer. The ratio of *rac*-*meso*-diastereomers in solution is solvent- and temperature-dependent, consistent with an intermolecular exchange between the diastereomers. An intramolecular dynamic phenomenon involving dissociation and recoordination of Mg–N bonds was also observed.

Introduction

In the last decade the dimethylaminomethylferrocenyl unit (FcN) has become an extremely versatile ligand for the synthesis of stable organometallic complexes containing metals from the entire periodic table. On the one hand the geometric properties of the ligand give rise to effective steric shielding and stabilization upon coordination to a metal, and, on the other hand, the ligand is flexible enough to adapt various coordination modes.[1] The most abundant coordination mode is (*C,N*)-bidentate, with the α-carbon atom from the substituted Cp-ring and the amine nitrogen as donors to the same metal (Figure 1), such as found in the following compounds: $(FcN)_2TlCl$,[2] $(FcN)SiCl_3$,[3] $(FcN)_2Pt$,[4] (FcN)PtCl(DMSO),[5] $(FcN)_2VCl$,[6] and $CpTi(FcN)Cl_2$.[6] The X-ray diffraction analyses of $Cp_2M(FcN)_2$ (M = Ti, Zr, Hf),[7] $Cp_2Ti(FcN)Cl$[6] and $(FcN)_2Yb(\mu\text{-}Cl)_2Li(THF)_2$ [8] revealed a monodentate *C*-bonded FcN. The FcN ligand can also act as a carbon bridging ligand, as found in $Li[Cp_2Y(FcN)_2]$,[9] $[(FcN)Cu]_4$ [10] and $[(FcN)Ag]_4$.[11] Another μ-(*C,N*)-bridging mode is found in $[(FcN)HgCl]_2$ [12] and $[(FcN)Au]_2$.[4] Some compounds show more than one coordination mode around the same metal, as, for instance, in the thallium compound $(FcN)_3Tl$,[13] with two bidentate and one monodentate FcN ligands. In solution, this compound appears to be dynamic, but this aspect was not well investigated. Recently, we investigated the dynamic behavior of the lead compound $(FcN)_2Pb$.[14] A rapid dissociation of one of the Pb−N bonds and recoordination occurs in solution, whereas in the solid state both FcN ligands are (*C,N*)-bidentate bonded.

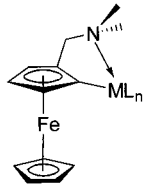

Figure 1. FcN as a bidentate ligand

The FcN ligand is chiral.[15] Therefore, when two or more FcN ligands are coordinated in one molecule this could give rise to the formation of diastereomers. Moreover, the chirality can be used as a "marker" to study intermolecular exchange processes, that could not have been observed otherwise. For instance, in the case of $(FcN)_2SiCl_2$ only the *meso*-form was found, whereas for $(FcN)_2SiMe_2$ both *rac*- and *meso*-diastereomers were formed, which could subsequently be separated by crystallization.[16] The silicon diastereomers obviously do not exchange. In contrast, for the first time, an intermolecular exchange between the diastereomers was demonstrated for $(FcN)_2Pb$.

Organomagnesium compounds, and in particular Grignard reagents, play an important role in organic synthesis. In order to explain the outcome and selectivity of alkylations with these compounds, it is of utmost importance to understand their structures in solution as well as in the solid state.[17,18] With this in mind, it was decided to use the FcN ligand for a thorough study of the structure and dynamics of this highly useful class of reagents.

[a] Institut für Anorganische Chemie der Martin-Luther-Universität Halle-Wittenberg,
Geusaer Straße 88, 06217 Merseburg, Germany
[b] Chemisches Institut der Otto-von-Guericke-Universität Magdeburg,
Universitätsplatz 2, 39106 Magdeburg, Germany
[c] Institut für Angewandte Physik, Technische Universität Bergakademie Freiberg,
Bernhard von Cotta Straße 4, 09596 Freiberg, Germany
[d] Dipartimento di Chimica dell'Università di Siena,
Pian dei Mantellini 44, I-53100 Siena, Italy

  1434−1948/01/0101−0145 $ 17.50+.50/0

Results and Discussion

The reaction of magnesium bromide with two equivalents of (FcN)Li,[19] in diethyl ether at room temperature, furnishes deep-red crystals of $[Li_2Mg(FcN)_2Br_2(OEt_2)_2]$ **(1)**, in 80% yield (Scheme 1). The same product is formed when the starting compounds are mixed in a ratio of 1:1; half of the $MgBr_2$ is left unchanged. Compound **1** may be considered as a trapped intermediate during the formation of the diorganomagnesium compounds $(FcN)_2Mg$ discussed below. It is interesting to note that in these and other reactions with (FcN)Li and MgX_2 no Grignard compounds (FcN)MgX are formed.[20]

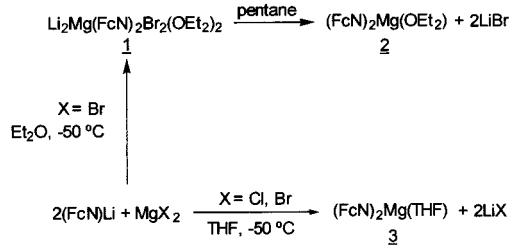

Scheme 1

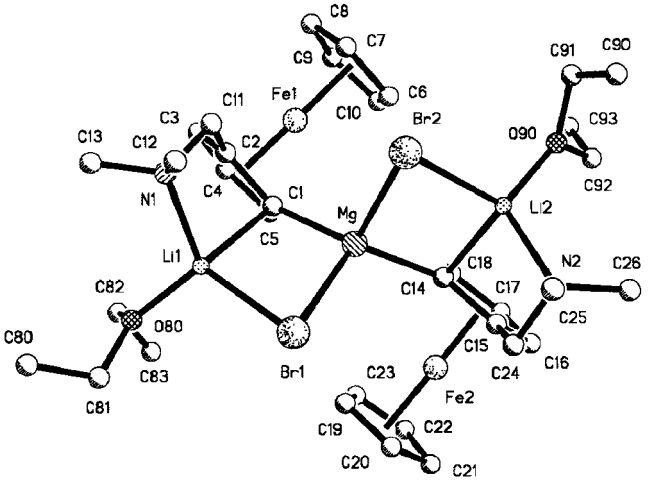

Figure 2. The molecular structure of **1**

Compound **1** crystallizes solely as a *rac*-diastereomer. The results of the X-ray diffraction analysis show that **1** is a magnesate compound where $Li(OEt_2)$ moieties are linked to the "$MgBr_2$" unit by *C*-bridging FcN groups. The molecular structure of **1** is shown in Figure 2 and the most important molecular dimensions are summarized in Table 1. The central magnesium atom shows a distorted tetrahedral coordination geometry with angles ranging from 98.06(4)°(Br1−Mg−Br2) to 119.8(2)° (C14−Mg−C1). The magnesium-bromide bond distances correspond approximately with the sum of the ionic radii of Br^- and Mg^{2+} [sum of ionic radii 263 pm,[21] Mg−Br1 = 260.08(13), Mg−Br2 = 260.52(13) pm]. The bromide-lithium bonds are somewhat shorter than the sum of the ionic radii [Br1−Li1 250.8(7), Br2−Li2 249.3(7) pm; sum of ionic radii 255 pm].[21] The lithium atoms are also four coordinate with angles ranging from 92.2(3)° (N1−Li1−C1) to 117.8(4)° (O80−Li1−C1) for Li1 and from 95.2(3)° (N2−Li2−C14) to 118.9(4)° (O90−Li2−N2) for Li2. The nitrogen atoms show an appreciable deviation from a tetrahedral geometry. The angles range from 97.1(3)° (C24−N2−Li2) to 118.2(3)° (C25−N2−Li2). The sum of the angles around the oxygens of the coordinating diethyl ether molecules is 359.5(5) [O80], and 359.0(4) pm [O90]. The best planes of the spiro system (Li1−C1−Mg−Br1, Li2−C14−Mg−Br1) are almost rectangular (82.6°).

Extraction of compound **1** with boiling pentane affords $[(FcN)_2Mg(OEt_2)]$ **(2)** in quantitative yield in the form of orange crystals (Scheme 1). The X-ray diffraction analysis of **2** (vide infra) reveals that the compound exists in the solid state as a *rac*-diastereomer.

Reaction of magnesium chloride with two equivalents of (FcN)Li and a small excess of tetrahydrofuran in ether furnishes orange crystals of $[(FcN)_2Mg(THF)]$ **(3)**, in 80% yield (see Scheme 1). The X-ray diffraction analysis shows that **3** also crystallizes as a *rac*-diastereomer. The alternative method of preparing **3** is from the reaction of magnesium

Table 1. Selected molecular dimensions in complex **1**; bond lengths [Å], angles [°] (ESDs are in parentheses)

Mg−C1	2.169(4)	Fe1−C(1m)[a]	1.653
Mg−C14	2.167(4)	Fe1−C(2m)	1.658
Li1−C1	2.390(8)	Fe2−C(3m)	1.642
Li2−C14	2.311(8)	Fe2−C(4m)	1.652
Mg−Li1	3.029(7)	Li1−N1	2.074(8)
Mg−Li2	2.994(7)	Li2−N2	2.065(7)
Mg−Br1	2.6008(13)	Li1−Br1	2.508(7)
Mg−Br2	2.6052(13)	Li2−Br2	2.493(7)
C1−Mg−C14	119.8(2)	Li1−O80	1.894(8)
Br1−Mg−Br2	98.06(4)	Li2−O90	1.911(7)
N1−Li1−C1	92.2(3)	N2−Li2−C14	95.2(3)
N1−Li1−Br1	113.2(3)	N2−Li2−Br2	109.5(39
O80−Li1−C1	117.8(4)	O90−Li2−C14	112.6(3)
O80−Li1−Br1	115.5(3)	O90−Li2−Br2	115.7(3)
Li1−N1−C(11−13)	99.8(3) to 117.5(4)	Li2−N2−C(24−26)	97.1(3) to 118.2(3)
Br1−Mg−C1−Li1	7.9(2)	Br2−Mg−C1−Li1	-92.3(2)
Br1−Mg−C14−Li2	104.9(2)	Br2−Mg−C14−Li2	1.2(2)

[a] The suffix 'm' denotes the centroid of a Cp ring.

bromide with two equivalents of (FcN)Li in a mixture of tetrahydrofuran and toluene.

The crystal structures of **2** and **3** are very similar, and therefore they will be discussed together, with parameters for compound **3** given in square brackets. Compound **2** crystallizes in the space group $P2_12_12_1$, and compound **3** in the space group $P2_1/n$. The X-ray structures of **2** and **3**, with their atomic numbering schemes, are shown in Figure 3 and 4. Bond distances and angles are given in Table 2. The crystal structures of both compounds are built up from discrete monomers. The magnesium atom is five-coordinate with two (*C,N*)-chelate-bonded FcN ligands and one *O*-bonded ether molecule in **2** (tetrahydrofuran in **3**). The coordination geometry shows a 59% [63%] distortion from a trigonal bipyramid towards a square pyramid along the Berry pseudorotation coordinate.[22] The distortion is defined by bending of the C1−Mg−C14 angle around the N1−Mg−N2 axis. The small bite angle of the FcN ligands (C−Mg−N ca 79°) causes distortions around the α-carbon atoms and nitrogen atoms. For instance, although the C−N−C angles have ideal values, the Mg−N1−C11 and Mg−N2−C24 angles {99.85(1) [100.90(3)] and 97.89(2)° [102.46(3)°], respectively} are smaller than the other Mg−N−C angles. Similarly, the C2−C1−Mg and C15−C14−Mg angles {110.1(1)° [110.8(2)°] and 110.0(2)° [111.1(2)°], respectively} are smaller than C5−C1−Mg and C18−C14−Mg angles {144.4(2) [144.2(2)] and 145.0(2)° [145.2(2)°], respectively}. The sum of the angles around the oxygen atom is 359.9(2)° [359.9(2)°], indicating an almost perfect trigonal geometry. The puckering in the tetrahydrofuran molecule in **3** is described as an envelope with C29 sticking out of the plane defined by the other four atoms in the ring.

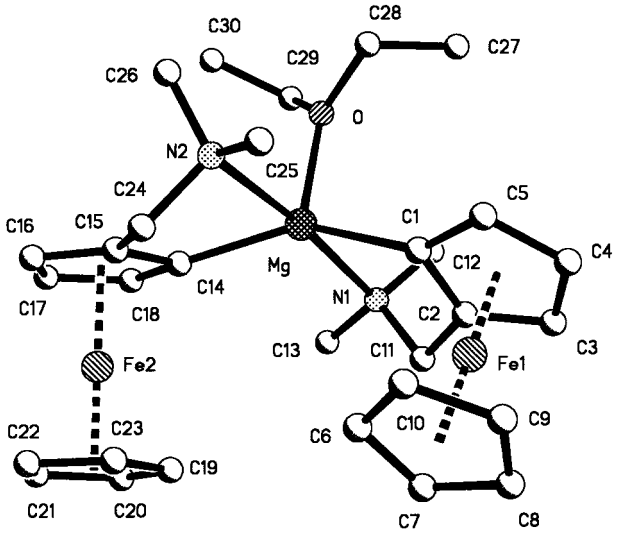

Figure 3. The molecular structure of **2**

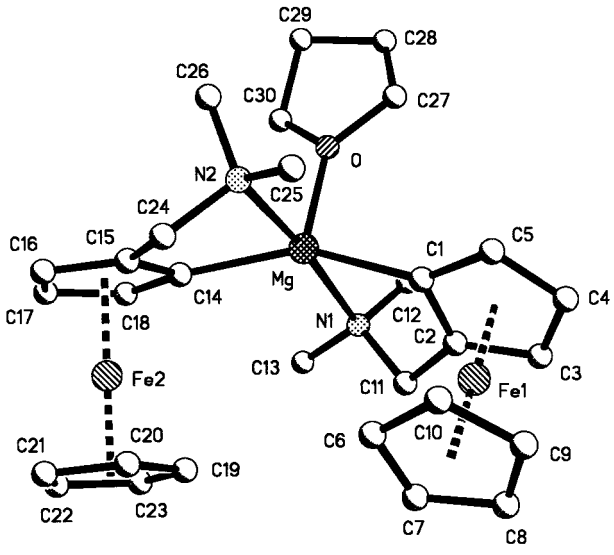

Figure 4. The molecular structure of **3**

The ^1H and ^{13}C NMR spectroscopic data in $[D_8]$THF at 21 °C of all three compounds are virtually identical and correspond to the solvated $(FcN)_2Mg$ species. The solution data show the presence of two diastereomers in a ratio of 3:1. In order to distinguish both diastereomers in solution, it occurred to us that **2**, as a chiral compound, crystallizes

Table 2. Selected molecular dimensions in complexes **2** and **3**; bond lengths [Å], angles [°] (ESDs are in parentheses)

	2	**3**		**2**	**3**
Mg−C1	2.150(2)	2.151(2)			
Mg−C14	2.152(2)	2.160(2)	Fe1−C(1m)[a]	1.652	1.648
Mg−N1	2.412(2)	2.421(2)	Fe1−C(2m)	1.658	1.657
Mg−N2	2.465(2)	2.419(2)	Fe2−C(3m)	1.652	1.656
Mg−O	2.084(2)	2.077(2)	Fe2−C(4m)	1.661	1.660
C1−Mg−C14	147.68(8)	150.59(9)	Mg−N1−C11	95.75(11)	100.80(13)
N1−Mg−N2	172.73(7)	172.34(7)	Mg−N2−C24	97.79(12)	102.36(13)
C1−Mg−O	105.35(7)	102.40(8)	C2−C1−Mg	110.14(13)	110.8(2)
C14−Mg−O	106.96(7)	107.01(8)	C15−C14−Mg	110.0(2)	111.1(2)
N1−Mg−O	94.37(6)	92.02(7)	C5−C1−Mg	144.4(2)	144.4(2)
N2−Mg−O	92.89(7)	95.63(7)	C18−C14−Mg	145.0(2)	145.2(2)
C1−Mg−N1	78.89(7)	78.07(8)	C14−Mg−N2	78.69(7)	78.00(8)
C11−N1	1.493(3)	1.488(3)	N1−C12	1.471(3)	1.474(3)
C24−N2	1.489(3)	1.484(3)	N1−C13	1.476(3)	1.467(3)
C11−N1−C(av.)	109.2(2)	109.2(2)	N2−C25	1.474(3)	1.475(3)
C24−N2−C(av.)	109.5(2)	109.4(2)	N2−C26	1.468(3)	1.474(3)

[a] The suffix 'm' denotes the centroid of a Cp ring.

in the asymmetrical space group $P2_12_12_1$. Therefore in a single crystal, compound **2** exists as either the (*R*,*R*)- or (*S*,*S*)-diastereomer, which should prevent the conversion into the *meso*-diastereomer in solution, and therefore result in only one set of signals in the NMR spectra. The ^{1}H NMR spectrum of one single crystal indeed revealed signals of only one compound. By comparison, it was deduced that these signals belong to the major diastereomer, indicating that the *rac*-diastereomer is prevalent in solution at room temperature.

The NMR spectroscopic data at room temperature show only one set of signals for both FcN groups in each diastereomer, indicating intramolecular exchange (Table 3). Below −20 °C in [D$_8$]THF the signals of the methyl groups of the *rac* diastereomer start to broaden; those of the *meso*-(FcN)$_2$Mg broaden at −40 °C. At −60 °C there are two signals for the methyl groups of *rac*-(FcN)$_2$Mg at δ = 2.25 and 2.95. This diastereomer has C_2-symmetry along the Mg−O axis and therefore both FcN ligands are equivalent and only two signals for the methyl groups are expected. In contrast, due to lack of symmetry, *meso*-(FcN)$_2$Mg should exhibit four signals for the methyl groups. At −90 °C we observed two broad signals at δ = 2.10 and 2.65, and it is likely that the signals of the *meso*-diastereomer have not reached decoalescence completely. The temperature-dependent NMR spectroscopic data could be explained by a rapid dissociation and recoordination of the Mg−N bonds.

The ratio of diastereomers measured in different solvents ([D$_8$]THF, [D$_8$]toluene, C$_6$D$_6$) is temperature dependent (at room temp. 2.8, 2.5, and 2, respectively). This suggests an intermolecular exchange between diastereomers. The proportion of the *rac*-diastereomer is higher at lower temperatures. This observation is reminiscent to those of the plumbylene compound (FcN)$_2$Pb, with the difference that, for the latter compound, the *meso*-diastereomer is prevalent. The equilibrium constant K (*rac*/*meso*) gradually changes from 2.8 at +25 °C to 12.0 at −90 °C in [D$_8$]THF. Plotting ln$K$ against 1/T (Van't Hoff plot) gives a straight line from which the thermodynamic parameters ΔH = −5.92 kJ mol^{-1} K^{-1} and ΔS = −12.1 J mol^{-1} K^{-1} were obtained (r = 0.9819).

The mechanistic pathway for the observed intermolecular exchange most likely involves electron-deficient three-center two-electron interactions (see Scheme 2). It invokes a simultaneous migration of two σ-bonded FcN groups through an intermediate with carbon-bridged FcN groups. Although this mechanism is very similar to that proposed for (FcN)$_2$Pb, it is fundamentally different. In the lead compound, exchange of FcN ligand probably proceeds via a preliminary Pb−Pb interaction, whereas for the magnesium compound such an interaction is highly unlikely.

The redox behavior of complex **3** has been examined by electrochemical techniques. At any rate, the appearance of a primary, single-stepped two-electron oxidation points out that the two ferrocene units do not communicate electronically each other.

Figure 5 shows the anodic cyclic voltammetric profile exhibited by complex **3** in dichloromethane solution.

The single-stepped two-electron oxidation at $E^{\circ\prime}$ = +0.41 V (accompanied with a yellow-to-blue color change) has features of chemical reversibility (at 0.05 Vs^{-1}: i_{pc}/i_{pa} = 0.9; ΔE_p = 70 mV, blue-to-yellow change). The blue color is typical of the formation of the ferrocenium cation.

The oxidation potential may be compared with that of FcNH ($E^{\circ\prime}$ = +0.38 V). After exhaustive two-electron oxidation-reduction it displays a reversible anodic process at

Table 3. ^{1}H NMR spectroscopic data for **2** in [D$_8$]THF

[a]		NMe_2	CH_2N	CpFe	C_5H_3
21 °C	*rac*-	2.55 (s, 12 H)	3.03 (d, 2 H, J = 14) 3.59 (d, 2 H, J = 14)	4.06 (s, 10 H)	3.84 (s, 2 H) 4.00 (s, 2 H) 4.13 (s, 2 H)
	meso-	2.42 (s, 12 H)	2.86 (d, 2 H, J = 13) 3.83 (d, 2 H, J = 13)	4.11 (s, 10 H)	3.88 (s, 2 H) 3.98 (s, 2 H)[b]
−90 °C	*rac*-	2.25 (s, 6 H) 2.95 (s, 6 H)	3.11 (d, 2 H, J = 14) 3.50 (d, 2 H, J = 14)	4.13 (s, 10 H)	4.11 (s)[b] 4.16 (s, 2 H)
	meso-	2.10 (s, br, 6 H) 2.65 (s, br, 6 H)	2.49 (d, 2 H, J = 13)[b]	4.16 (s, 10 H)	3.92 (s, 2 H) 4.07 (s, br, 4 H)[b]

[a] The ^{1}H NMR spectroscopic data of **1** and **3** are virtually identical. − [b] Not all signals were observed, due to the overlap with other signals.

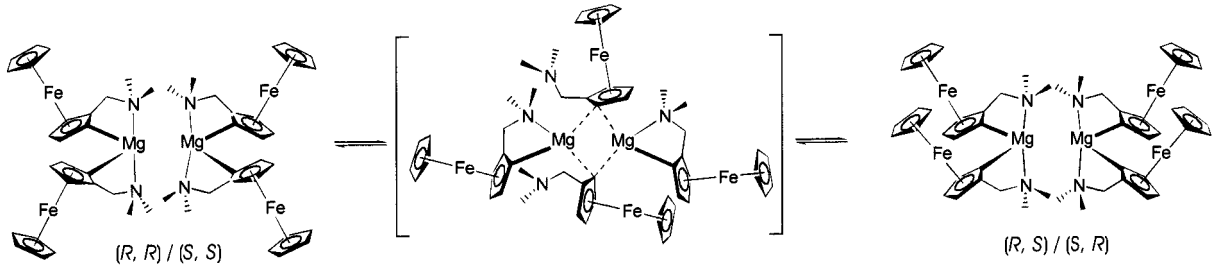

Scheme 2

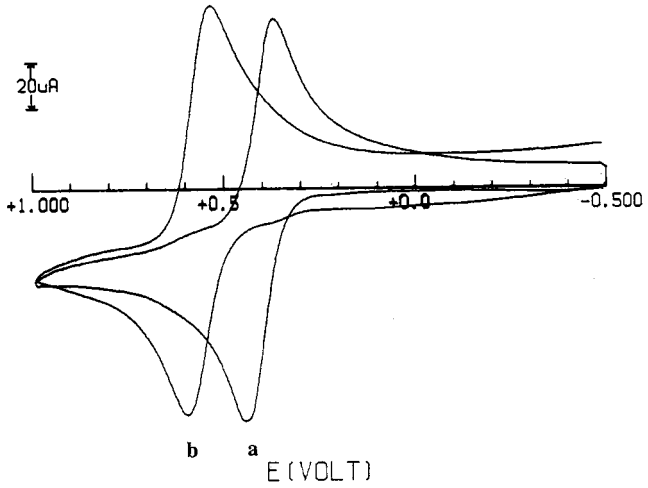

Figure 5. Cyclic voltammograms recorded on a platinum electrode in CH_2Cl_2 solution containing **1** (1.8×10^{-3} mol dm^{-3}) and $[NBu_4][PF_6]$ (0.2 mol dm^{-3}) before (a) and after (b) a cycle of exhaustive oxidation and reduction

$E^{\circ\prime}$ = +0.57 V (at 0.05 Vs^{-1}: ΔE_p = 76 mV), indicating decomposition of the compound (Figure 5b).

The Mössbauer parameters of **1** and **3** are shown in Table 4. The isomer shifts do not differ significantly from those of (FcN)Li,[23] titanium or vanadium compounds.[6]

Table 4. Mössbauer parameters for compounds **1** and **3** (78 K, referenced against α-iron foil)

Compound[a]	δ[b] [mm s^{-1}]	q.s.[c] [mm s^{-1}]	Γ[d] [mm s^{-1}]
1	0.520(2)	2.367(4)	0.324(7)
2	0.485(7)	2.33(2)	0.36(2)

[a] Numbers in parentheses correspond to the experimental error in the last significant figures. – [b] Isomer shift. – [c] Quadrupole splitting. – [d] Half-width at half height.

The data in Table 4 show lower values of *q.s.* for measured compounds relative to the *q.s.* in ferrocene [2.40(3) mm s^{-1}].[23] Such a decrease in *q.s.* is associated with electron-withdrawing substituents on the ferrocenyl moieties, and may be due to the binding of the Mg units to the FcN ligand. Nevertheless, this change is very small, indicating that the Fe^{II} orbitals are not very sensitive to ring substituents.

Conclusions

The diorganomagnesium compounds **1**–**3** are highly dynamic in solution. Although all three compounds only crystallize as (*C,N*)-bonded *rac*-diastereomers, a mixture of *meso*- and *rac*-diastereomers forms in solution. The *rac*/*meso*-ratio is solvent- and temperature-dependent, and consistent with an intermolecular exchange between diastereomers. An intramolecular dynamic process of dissociation and recoordination of Mg–N bonds is responsible for the equivalency of both FcN groups in solution.

Experimental Section

General Remarks: All experiments were carried out using standard Schlenk techniques under purified argon atmosphere. Solvents were distilled from sodium benzophenone ketyl prior to use. The commercial products *n*-butyllithium (1.6 M solution in hexane), magnesium chloride, magnesium bromide and dimethylaminomethylferrocenylferrocene were used without further purification. The known starting material (FcN)Li was prepared according to the literature.[19] – ^{1}H and ^{13}C NMR spectra were recorded on a Varian Unity 500 spectrometer. – Materials and apparatus for electrochemistry have been described elsewhere.[24] All potential values are referred to the Saturated Calomel Electrode (SCE). Under the present experimental conditions {dichloromethane solution containing $[NBu_4][PF_6]$ (0.2 mol dm^{-3})} the one-electron oxidation of ferrocene occurs at $E^{\circ\prime}$ = + 0.38 V. – Mössbauer data were recorded at 78 K on a Wissel spectrometer with a ^{57}Co source in a rhodium matrix, 1.8 GBq.

Synthesis of $[Li_2Mg(FcN)_2Br_2(OEt_2)_2]$ (1): (FcN)Li (5.00 g, 20.1 mmol) was added to a suspension of $MgBr_2$ (1.84 g, 10.0 mmol) in diethyl ether (150 mL) at −50 °C with vigorous stirring. After 1 h the reaction mixture was allowed to warm to room temperature whilst stirring, affording a clear orange-colored solution. The volume of the solution was reduced to the point of crystallization after one day and stored at 7 °C to give product **1** as orange air- and moisture-sensitive crystals. Yield: 6.64 g, 80%. – $C_{34}H_{52}Br_2Fe_2Li_2MgN_2O_2$ (830.49): calcd. C 49.17, H 6.31, N 3.37, Br 19.24; found C 49.21, H 6.35, N 3.32, Br 19.31. – ^{1}H NMR ([D$_8$]THF, room temp.; *meso*-diastereomer in square brackets): δ = 2.57 (s, 12 H, NMe_2) [2.42 (s, 12 H, NMe_2)], 3.03 (d, $^1J_{C,H}$ = 14 Hz, 2 H, CH_2N) [2.85 (d, $^1J_{C,H}$ = 13 Hz, 2 H, CH_2N], 3.60 (d, $^1J_{C,H}$ = 14 Hz, 2 H, CH_2N) [3.83 (d, $^1J_{C,H}$ = 13 Hz, 2 H, CH_2N], 4.06 (s, 10 H, C_5H_5) [4.11 (s, 10 H, C_5H_5)], 3.83 (s, 2 H, C_5H_3) [3.88 (s, 2 H, C_5H_3)], 3.99 (s, 2 H, C_5H_3) [3.97 (s, 4 H, C_5H_3)], 4.12 (s, 2 H, C_5H_3).

Synthesis of $[(FcN)_2Mg(OEt_2)]$ (2): Crystals of **1** were filtered off, and exhaustively extracted with pentane. The pentane solution was stored in a freezer at −30 °C to give product **2** as deep-reddish air- and moisture-sensitive crystals. Yield: 5.31 g, 80%. – $C_{30}H_{42}Fe_2MgN_2O$ (582.67): calcd. C 61.84, H 7.26, N 4.81; found C 61.92, H 7.32, N 4.75. – ^{13}C{^{1}H} NMR ([D$_8$]THF, room temp.; *meso*-diastereomer in square brackets): δ = 47.1 [46.7] (NMe_2), 63.0 [63.4] ($-CH_2N$), 76.5 [77.2] ($C_5H_3-CH_2NMe_2$), 95.4 [95.0] (C_5H_3-Mg).

Synthesis of $[(FcN)_2Mg(THF)$ (3)]: (FcN)Li (2.90 g, 11.6 mmol) was added to a suspension of $MgBr_2$ (1.07 g, 5.8 mmol) in 150 mL of toluene and 5 mL tetrahydrofuran at −78 °C with constant stirring. The orange-colored reaction mixture was stirred for 24 h. Workup as for **2**. Deep-reddish crystals of **3** were obtained after cooling the pentane solution to −30 °C. Yield: 2.93 g, 85%. – $C_{30}H_{40}Fe_2MgN_2O$ (580.65): calcd. C 62.05, H 6.94, N 4.83; found C 61.98, H 6.89, N 4.90. – ^{1}H NMR ([D$_8$]THF, room temp.; *meso*-diastereomer in square brackets): δ = 2.55 (s, 12 H, NMe_2) [2.42 (s, 12 H, NMe_2)], 3.03 (d, $^1J_{C,H}$ = 14 Hz, 2 H, CH_2N) [2.86 (d, $^1J_{C,H}$ = 13 Hz, 2 H, CH_2N)], 3.59 (d, $^1J_{C,H}$ = 13 Hz, 2 H, CH_2N) [3.83 (d, $^1J_{C,H}$ = 13 Hz, 2 H, CH_2N)], 4.06 (s, 10 H, C_5H_5) [4.11 (s, 10 H, C_5H_5)], 3.84 (s, 2 H, C_5H_3) [3.88 (s, 2 H, C_5H_3)], 4.00 (s, 2 H, C_5H_3) [3.98 (s, 4 H, C_5H_3)], 4.13 (s, 2 H, C_5H_3).

X-ray Structure Analyses of 1, 2 and 3: Crystal and numerical data of the structure determinations are given in Table 5. Crystals were covered with inert oil and mounted on a glass fiber, and then trans-

Table 5. Crystallographic data for **1**, **2** and **3**

	1	**2**	**3**
Empirical formula	$C_{34}H_{52}Br_2Fe_2Li_2MgN_2O_2$	$C_{30}H_{42}Fe_2MgN_2O$	$C_{30}H_{40}Fe_2MgN_2O$
Molecular mass	830.49	582.67	580.65
Crystal dimensions [mm]	0.80 × 0.50 × 0.40	0.55 × 0.50 × 0.16	0.40 × 0.24 × 0.12
Crystal system	monoclinic	orthorhombic	monoclinic
Space group	*C2/c*	$P2_12_12_1$	$P2_1/n$
a [Å]	34.3791(5)	10.4576(4)	12.2948(2)
b [Å]	11.2325(2)	11.3446(4)	10.59530(10)
c [Å]	22.3681(4)	24.1390(7)	21.8177(2)
α [°]	90	90	90
β [°]	115.8970(10)	90	97.7310(10)
γ [°]	90	90	90
V [Å^3]	7770.3(2)	2863.8(2)	2816.29(6)
Z	8	4	4
$d_{calcd.}$ [g cm^{-3}]	1.420	1.351	1.369
T [K]	173(2)	173(2)	163(2)
μ [mm^{-1}]	2.850	1.060	1.078
θ_{max} [°]	28.3	28.3	28.2
No. rflns.	25637	19229	18512
No. unique rflns.	9545	6994	6925
No. rflns. observed	6132	6183	5173
Structure determination	Direct methods	Direct methods	Direct methods
Refinement	on F^2 in SHELXL	on F^2 in SHELXL	on F^2 in SHELXL
No. parameters refined	414	332	329
$R_1[I > 2\sigma(I)]$	0.0529	0.0587	0.0395
wR_2 (all data)	0.1282	0.0627	0.0846
Goodness-of-fit (on F^2)	1.017	1.084	1.046

ferred to the diffractometer in a stream of a cold gas (Bruker AXS Smart CCD System with LT-2 low-temperature adapter). Monochromatic Mo-K_α radiation (λ = 71.073 pm) was used. Data were corrected for Lorentz and polarization effects. Absorption correction (multi-scan method SADABS) was employed. The structures were solved by direct methods using the SHELXS program and refined by full-matrix least-squares against F^2 with SHELXL-97.[25] All non-hydrogen atoms were refined with anisotropic thermal parameters. All hydrogen atoms were found in the difference Fourier map and refined isotropically.

Crystallographic data (excluding structure factors) for the reported structures have been deposited with the Cambridge Crystallographic Data Centre as supplementary publication no. CCDC-113801 (**1**), -113802 (**2**), -113803 (**3**). Copies of data can be obtained free of charge on application to CCDC, 12 Union Road, Cambridge CB2 1EZ, UK [Fax: (internat.) +44-1223/336-093; E-mail: deposit@ccdc.cam.ac.uk].

Acknowledgments

N. S. thanks Dr. Adolphus A. H. van der Zeijden for fruitful discussions. K. J. thanks the Deutsche Forschungsgemeinschaft DFG for financial support, N. S. thanks the DFG program "Graduierten-Kolleg: Synthese und Reaktionsverhalten von Organometallverbindungen und Metallkomplexen" for a fellowship, P. Z. thanks University of Siena for financial support (ex-quota 60%).

[1] F. T. Edelmann, K. Jacob, *J. Prakt. Chem.* **1998**, *340*, 393−407.
[2] K. Jacob, J. Scholz, K. Merzweiler, C. Pietzsch, *J. Organomet. Chem*. **1997**, *527*, 109−115.
[3] W. Palitzsch, C. Pietzsch, K. Jacob, F. T. Edelmann, T. Gelbrich, V. Lorenz, M. Puttnat, G. Roewer, *J. Organomet. Chem*. **1998**, *554*, 139−146.
[4] K. Jacob, F. Voigt, K. Merzweiler, C. Pietzsch, *J. Organomet. Chem*. **1997**, *545−546*, 421−433.
[5] P. Ramani R. Ranatunge-Bandarage, B. H. Robinson, J. Simpson, *Organometallics* **1994**, *13*, 500−510.
[6] P. B. Hitchcock, D. L. Hughes, G. J. Leigh, J. R. Sanders, J. S. de Souza, *J. Chem. Soc., Dalton Trans.* **1999**, 1161−1174.
[7] K.-H. Thiele, C. Krüger, R. Boese, G. Schmid, T. Bartik, G. Pályi, *Z. Anorg. Allg. Chem*. **1990**, *590*, 55−64.
[8] H. Gornitzka, A. Steiner, D. Stalke, U. Kilimann, F. T. Edelmann, K. Jacob, K.-H. Thiele, *J. Organomet. Chem*. **1992**, *439*, C6−C10.
[9] K. Jacob, M. Schäfer, A. Steiner, G. M. Sheldrick, F. T. Edelmann, *J. Organomet. Chem*. **1995**, *487*, C18−C20.
[10] A. Nesmeyanov, Yu. T. Struchkov, N. N. Sedova, V. G. Andrianov, Yu. V. Volgin, V. A. Sazonova, *J. Organomet. Chem*. **1977**, *137*, 217−221.
[11] A. Nesmeyanov, N. N. Sedova, Yu. T. Struchkov, V. G. Andrianov, E. N. Stakheeva, V. A. Sazonova, *J. Organomet. Chem*. **1978**, *153*, 115−122.
[12] L. G. Kuz'mina, Yu. T. Struchkov, D. A. Lemenovskii, I. F. Urasovskii, I. E. Nifanev, L. G. Perevalova, *Koord. Khim*. **1983**, *9*, 1212−1219.
[13] K. Jacob, J. Scholz, C. Pietzsch, F. T. Edelmann, *J. Organomet. Chem*. **1995**, *501*, 71−77.
[14] N. Seidel, K. Jacob, A. A. H. van der Zeijden, H. Menge, K. Merzweiler, C. Wagner, *Organometallics* **2000**, *19*, 1438−1441.
[15] K. Schlögl , M. Fried, *Monatsh. Chem*. **1964**, *95*, 558−575.
[16] W. Palitzsch, C. Pietzsch, M. Puttnat, K. Jacob, K. Merzweiler, P. Zanello, A. Cinquantini, M. Fontani, G. Roewer, *J. Organomet. Chem*. **1999**, *587*, 9−17.
[17] V. C. R. Grignard, *Hebd. Seances Acad. Sci*. **1900**, *130*,1322.
[18] P. R. Markies, O. S. Akkerman, F. Bickelhaupt, W. J. J. Smeets, A. L. Spek, *Adv. Organomet. Chem.* **1991**, *32*, 147−226.
[19] M. D. Rausch, G. A. Moser, C. F. Maede, *J. Organomet. Chem*. **1973**, *51*, 1−12.
[20] The Grignard compound (FcN)MgBr can be obtained by reaction of $(FcN)_2Mg$ and $MgBr_2$ in ether. (FcN)MgBr was preliminary characterized by ^1H and ^{13}C NMR spectroscopy. In the Schlenk-type equilibrium the Grignard compound is obviously favored. N. Seidel, K. Jacob, *Unpublished results.*
[21] *CRC Handbook of Chemistry and Physics*, 78th Edition, CRC Press, Boca Raton, New York **1997**, Section 12−14.
[22] R. R. Holmes, *Prog. Inorg. Chem*. **1984**, *32*, 119−236.
[23] K. Jacob, W. Palitzsch, *Z. Anorg. Allg. Chem*. **1994**, *620*, 1489−1493.

[24] A. Togni, M. Hobi, G. Rihs, G. Rist, A. Albinati, P. Zanello, D. Zech, H. Keller, *Organometallics* **1994**, *13*, 1224−1234.
[25] G. M. Sheldrick, SHELXS, *Program for Crystal Structure Determination*, University of Göttingen, Germany, **1986**; SHELXL-97, *Program for Crystal Structure Refinement*, University of Göttingen, Germany, **1997**.

Received May 23, 2000
[I00201]